

On Boolean gates in fungal colony

Andrew Adamatzky^{a,b}, Martin Tegelaar^c, Han A. B. Wosten^c,
Anna L. Powell^a, Alexander E. Beasley^a, Richard Mayne^{a,d}

^a*Unconventional Computing Laboratory, UWE, Bristol, UK*

^b*Corresponding author: andrew.adamatzky@uwe.ac.uk*

^c*Microbiology Department, University of Utrecht, Utrecht, The Netherlands*

^d*Department of Applied Sciences, University of the West of England, UWE, Bristol, UK*

Abstract

A fungal colony maintains its integrity via flow of cytoplasm along mycelium network. This flow, together with possible coordination of mycelium tips propagation, is controlled by calcium waves and associated waves of electrical potential changes. We propose that these excitation waves can be employed to implement a computation in the mycelium networks. We use FitzHugh-Nagumo model to imitate propagation of excitation in a single colony of *Aspergillus niger*. Boolean values are encoded by spikes of extracellular potential. We represent binary inputs by electrical impulses on a pair of selected electrodes and we record responses of the colony from sixteen electrodes. We derive sets of two-inputs-on-output logical gates implementable the fungal colony and analyse distributions of the gates.

Keywords: mycelium network, Boolean gates, unconventional computing

1. Introduction

A vibrant field of unconventional computing aims to employ space-time dynamics of physical, chemical and biological media to design novel computational techniques, architectures and working prototypes of embedded computing substrates and devices. Interaction-based computing devices, is one of the most diverse and promising families of the unconventional computing structures. They are based on interactions of fluid streams, signals propagating along conductors or excitation wave-fronts, see e.g. [67, 64, 10, 10, 81, 76, 37, 29, 30, 70, 27, 73, 70, 31]. Typically, logical gates and their cascade implemented in an excitable medium are ‘handcrafted’

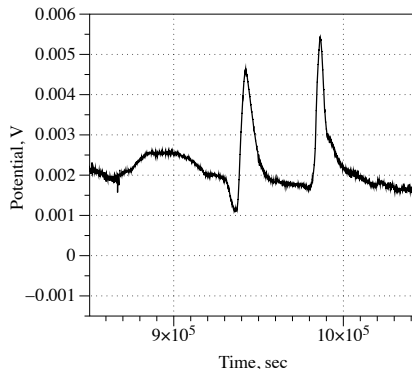


Figure 1: Exemplar spikes of extracellular electrical potential propagating in fungal mycelium.

to address exact timing and type of interactions between colliding wavefronts [67, 64, 1, 9, 74, 8, 20, 71, 82, 72, 32, 7, 69]. The artificial design of logical circuits might be suitable when chemical media or functional materials are used. However, the approach might be not feasible when embedding computation in living systems, where the architecture of conductive pathways may be difficult to alter or control. In such situations an opportunistic approach to outsourcing computation can be adopted. The system is perturbed via two or more input loci and its dynamics if recorded at one or more output loci. A wave-front appearing at one of the output loci is interpreted as logical truth or ‘1’. Thus the system with relatively unknown structure implements a mapping $\{0, 1\}^n \rightarrow \{0, 1\}^m$, where n is a number of input loci and m is a number of output loci, $n, m > 0$ [12, 6]. The approach belong to same family of computation outsourcing techniques as *in materio* computing [47, 48, 68, 49, 50] and reservoir computing [77, 43, 18, 42, 19].

Fungal colonies are characterised by rich typology of mycelium networks [36, 28, 23, 24, 38] in some cases affine to fractal structures [53, 56, 16, 46, 15, 55]. Rich morphological features might imply rich computational abilities and thus worse to analyse from realising Boolean functions point of view. In numerical experiments we study implementation of logical gates via interaction of numerous travelling excitation waves, seen as as action potentials, on an image of a real fungal colony. Action potential-like spikes of electrical potential have been discovered using intra-cellular recording of mycelium of *Neurospora crassa* [66] and further confirmed in intra-cellular recordings of action potential in hypha of *Pleurotus ostreatus* and *Armillaria bulbosa* [54]

and in extra-cellular recordings of fruit bodies of and substrates colonized by mycelium of *Pleurotus ostreatus* [4] (Fig. 1). While the exact nature of the travelling spikes remains uncertain we can speculate, by drawing analogies with oscillations of electrical potential of slime mould *Physarum polycephalum* [39, 40, 41, 45], that the spikes in fungi are triggered by calcium waves, reversing of cytoplasmic flow, translocation of nutrients and metabolites. Studies of electrical activity of higher plants can bring us even more clues. Thus, the plants use the electrical spikes for a long-distance communication aimed to coordinate an activity of their bodies [75, 26, 83]. The spikes of electrical potential in plants relate to a motor activity [65, 25, 63, 80], responses to changes in temperature [51], osmotic environment [79] and mechanical stimulation [59, 58]. The paper is structured as follows. Colony imaging and numerical solutions of FitzHugh-Nagumo equations are introduced in Sect. 2. Section 3 studies a role of excitability on the coverage of the network by travelling waves of excitation and exemplifies distributions of Boolean computable on the given mycelium network. We discuss operation characteristics of the mycelium computer in Sect. 4.

2. Methods

2.1. Colony imaging

Aspergillus niger strain AR9#2 [78], expressing Green Fluorescent Protein (GFP) from the glucoamylase (*glaA*) promoter, was grown at 30°C on minimal medium (MM) [21] with 25 mM xylose and 1.5% agarose (MMXA). MMXA cultures were grown for three days, after which conidia were harvested using saline-Tween (0.8% NaCl and 0.005% Tween-80). 250 ml liquid cultures were inoculated with $1.25 \cdot 10^9$ freshly harvested conidia and grown at 200 rpm and 30°C in 1 L Erlenmeyer flasks in complete medium (CM) (MM containing 0.5% yeast extract and 0.2% enzymatically hydrolyzed casein) supplemented with 25 mM xylose (repressing *glaA* expression). Mycelium was harvested after 16 h and washed twice with PBS. Ten g of biomass (wet weight) was transferred to MM supplemented with 25 mM maltose (inducing *glaA* expression).

Fluorescence of GFP was localised in micro-colonies using a DMI 6000 CS AFC confocal microscope (Leica, Mannheim, Germany). Micro-colonies were fixed overnight at 4°C in 4% paraformaldehyde in PBS, washed twice with PBS and taken up in 50 ml PBS supplemented with 150 mM glycine to

quench autofluorescence. Micro-colonies were then transferred to a glass bottom dish (Cellview™, Greiner Bio-One, Frickenhausen, Germany, PS, 35/10 MM) and embedded in 1% low melting point agarose at 45°C. Micro-colonies were imaged at 20× magnification (HC PL FLUOTAR L 20 × 0.40 DRY). GFP was excited by white light laser at 472 nm using 50% laser intensity (0.1 kW/cm²) and a pixel dwell time of 72 ns. Fluorescent light emission was detected with hybrid detectors in the range of 490–525 nm. Pinhole size was 1 Airy unit. Z-stacks of imaged micro-colonies were made using 100 slices with a slice thickness of 8.35 μm. 3D projections were made with Fiji [62].

2.2. Numerical modelling

We used still image of the colony as a conductive template. The image of the fungal colony (Fig. 2a) was projected onto a 1000 × 960 nodes grid. The original image $M = (m_{ij})_{1 \leq j \leq n_i, 1 \leq i \leq n_j}$, $m_{ij} \in \{r_{ij}, g_{ij}, b_{ij}\}$, where $n_i = 1000$ and $n_j = 960$, and $1 \leq r, g, b \leq 255$ (Fig. 2a), was converted to a conductive matrix $C = (m_{ij})_{1 \leq i, j \leq n}$ (Fig. 2b) derived from the image as follows: $m_{ij} = 1$ if $r_{ij} < 20$, ($g_{ij} > 40$) and $b_{ij} < 20$; a dilution operation was applied to C .

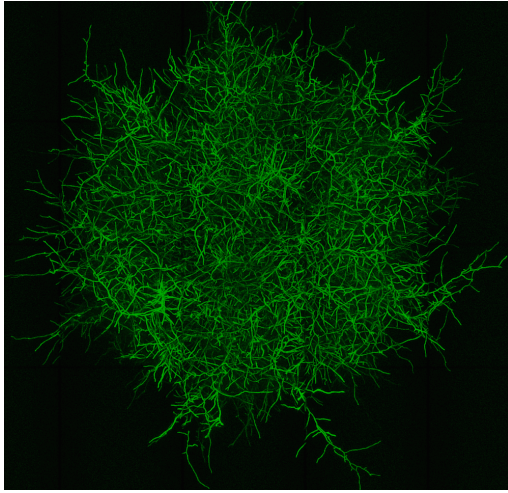
FitzHugh-Nagumo (FHN) equations [22, 52, 57] is a qualitative approximation of the Hodgkin-Huxley model [14] of electrical activity of living cells:

$$\frac{\partial v}{\partial t} = c_1 u(u - a)(1 - u) - c_2 uv + I + D_u \nabla^2 \quad (1)$$

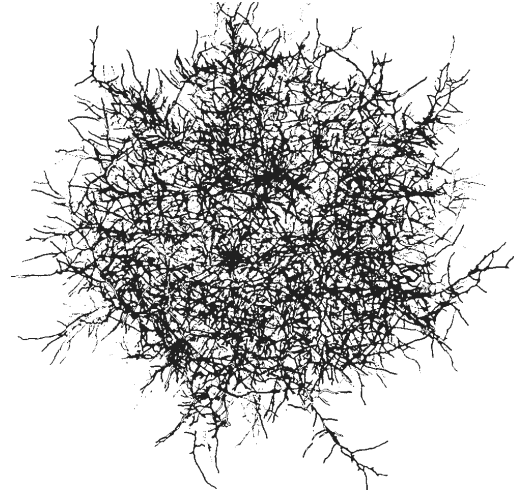
$$\frac{\partial v}{\partial t} = b(u - v), \quad (2)$$

where u is a value of a trans-membrane potential, v a variable accountable for a total slow ionic current, or a recovery variable responsible for a slow negative feedback, I is a value of an external stimulation current. The current through intra-cellular spaces is approximated by $D_u \nabla^2$, where D_u is a conductance. Detailed explanations of the ‘mechanics’ of the model are provided in [60], here we shortly repeat some insights. The term $D_u \nabla^2 u$ governs a passive spread of the current. The terms $c_2 u(u - a)(1 - u)$ and $b(u - v)$ describe the ionic currents. The term $u(u - a)(1 - u)$ has two stable fixed points $u = 0$ and $u = 1$ and one unstable point $u = a$, where a is a threshold of an excitation.

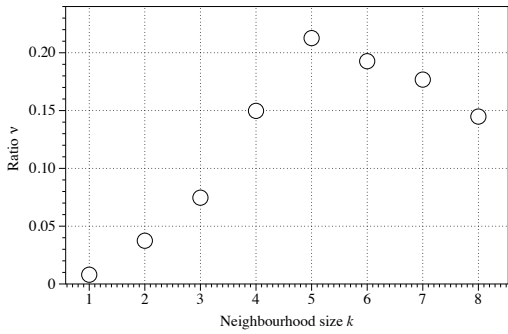
We integrated the system using the Euler method with the five-node Laplace operator, a time step $\Delta t = 0.015$ and a grid point spacing $\Delta x = 2$, while other parameters were $D_u = 1$, $a = 0.13$, $b = 0.013$, $c_1 = 0.26$. We controlled excitability of the medium by varying c_2 from 0.05 (fully excitable)



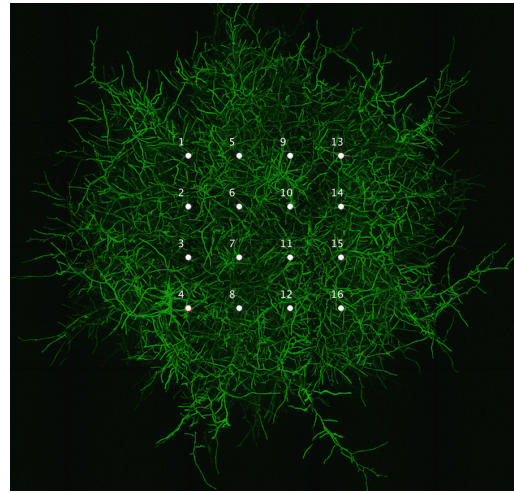
(a)



(b)



(c)



(d)

Figure 2: Image of the fungal colony, 1000×960 pixels used as a template conductive for FHN. (a) Original image, mycelium is seen as green pixels. (b) Conductive matrix C , conductive pixels are black. (c) Distribution of neighbourhood sizes. (d) Configuration of electrodes.

to 0.015 (non excitable). Boundaries are considered to be impermeable: $\partial u / \partial \mathbf{n} = 0$, where \mathbf{n} is a vector normal to the boundary.

The waves of excitation propagated on conductive nodes of the grid of C , in addition to the parameter c_2 , excitability of each conductive node was dependent on a number k of its immediate conductive neighbours. Distribution of neighbourhood sizes are shown in Fig. 2c.

To show dynamics of excitation in the network we simulated electrodes by calculating a potential p_x^t at an electrode location x as $p_x = \sum_{y:|x-y|<2} (u_x - v_x)$. Configuration of electrodes 1, \dots , 16 is shown in Fig. 2d. The numerical integration code written in Processing was inspired by previous methods of numerical integration of FHN and our own computational studies of the impulse propagation in biological networks [33, 57, 60, 5, 6]. Time-lapse snapshots provided in the paper were recorded at every 100th time step, and we display sites with $u > 0.04$; videos and figures were produced by saving a frame of the simulation every 100th step of the numerical integration and assembling the saved frames into the video with a play rate of 30 fps. Videos are available at [13].

3. Results

While implementing numerical experiments were selected a range the network excitability (Subsect. 3.1) and then realised sets of logical gates for excitability values selected (Subsect. 3.2).

3.1. Effect of excitability on overall activity

For $c_2 < 0.0945$ any source of excitation triggers excitation dynamics which occupies all parts of the network accessible, via mycelial strands, from the source. Due to the high level of excitability the network remains in the excitable state (Fig. 3a). For values c_2 from 0.094 to 0.00965 we observe propagation of ‘classical’ excitation wave-fronts resembling circular, target and spiral waves in a continuous medium. Examples of wave-fronts propagating in networks with excitability levels $c_2 = 0.095$ and $c_2 = 0.096$, excited at the same loci shown in Fig. 4a, are shown in Figs.4 and 5. In the network with c_2 there are many pathways for propagation of the excitation wave-fronts, therefore, despite being fully deterministic, the network exhibit disordered oscillations of its activity (Fig. 3c). A number of conductive pathways decreases when c_2 increases from 0.095 to 0.096. Thus many propagating wave-fronts become, relatively, quickly confined to a limited domains of the

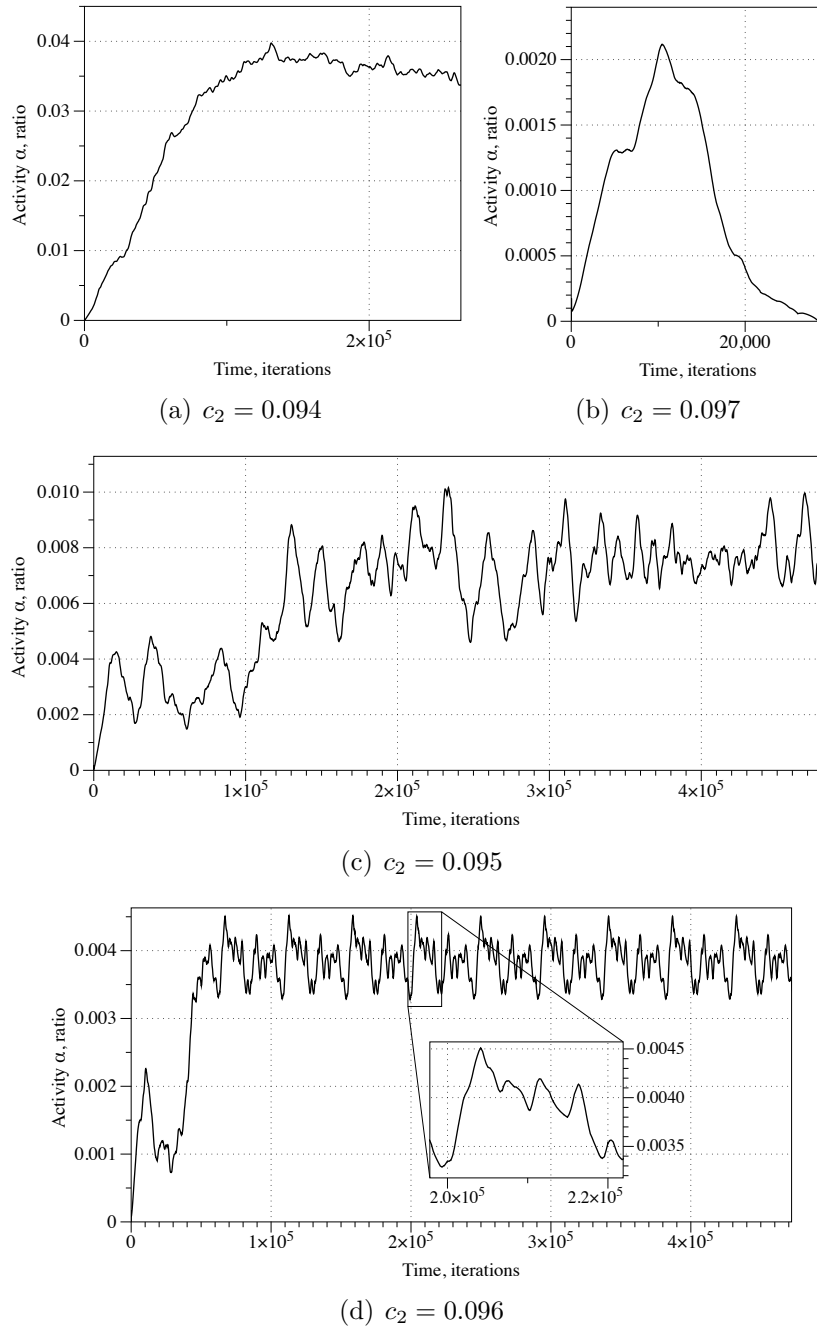


Figure 3: Dynamics of the activity α for various values of excitability c_2 , the values are shown in sub-captions. For every iteration t we measured the activity of the network as a number of conductive nodes x with $u_x^t > 0.1$.

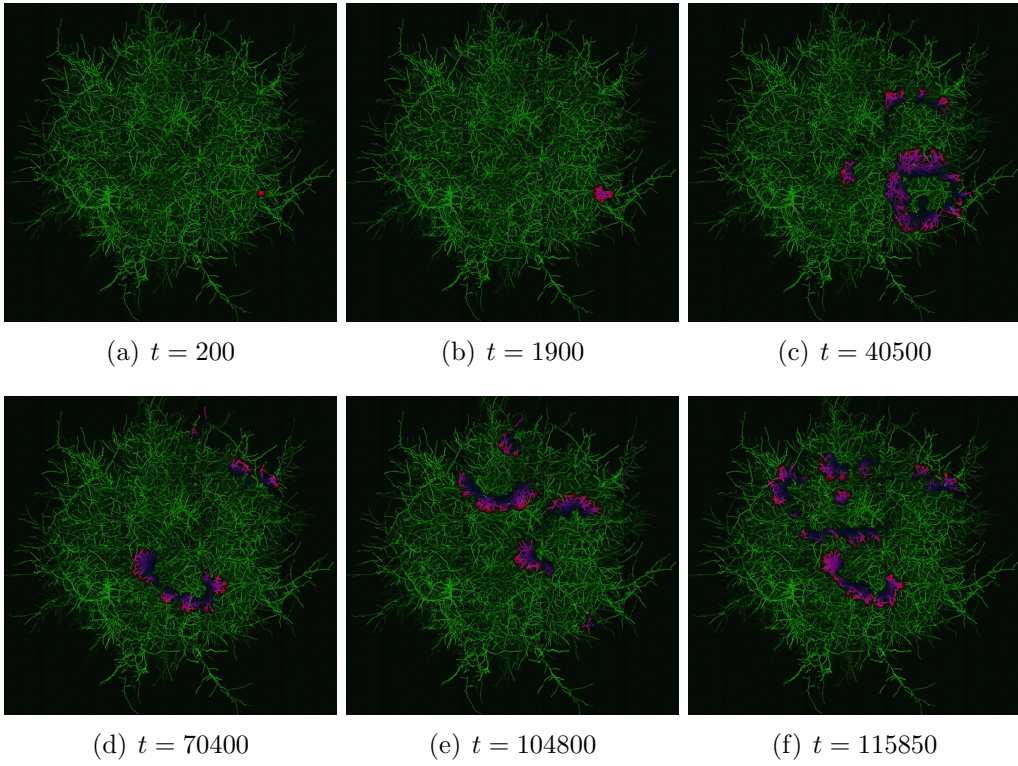


Figure 4: Snapshots of excitation dynamics for $c_2 = 0.095$.

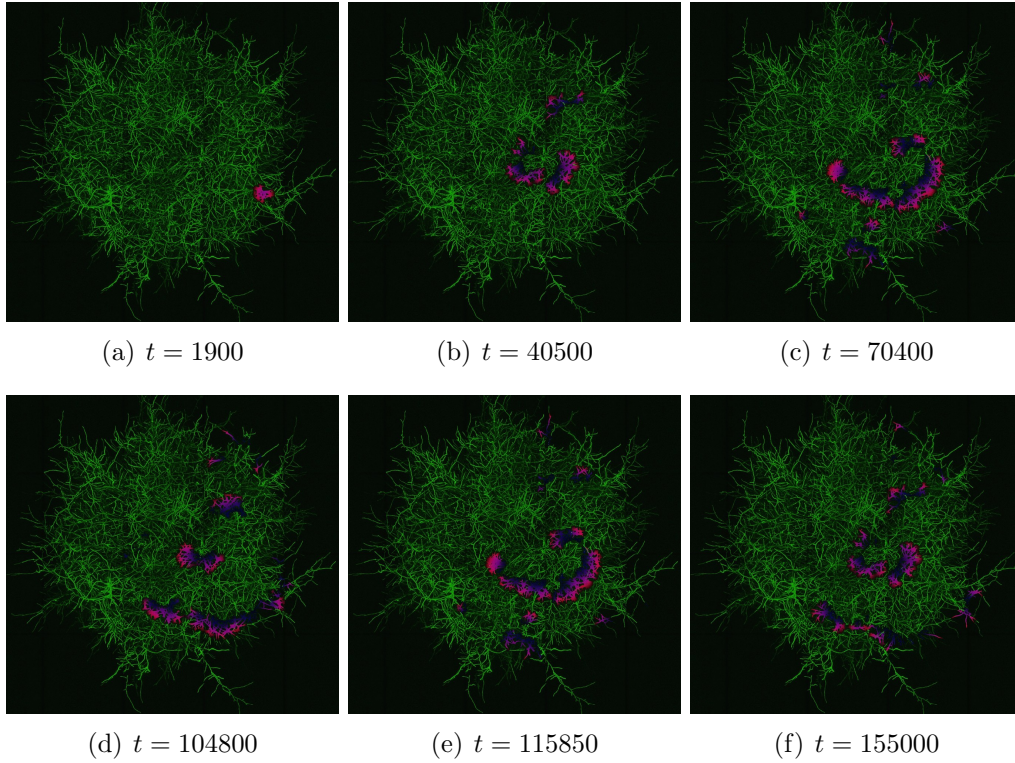


Figure 5: Snapshots of excitation dynamics for $c_2 = 0.096$. Compare (c) and (e): the pattern of excitation returns to the exact point of the cycle.

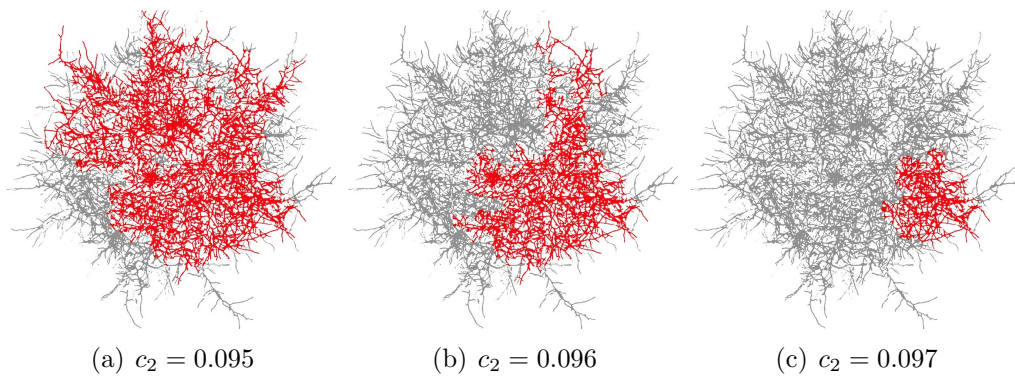


Figure 6: Coverage of the network for excitability c_2 (a) 0.095, (b) 0.096, (c) 0.097. If the a pixel p of the image was excited, $u_p^t > 0.1$, it is assumed to be covered and coloured red in the pictures (abc); the pixels which never were excited are coloured gray.

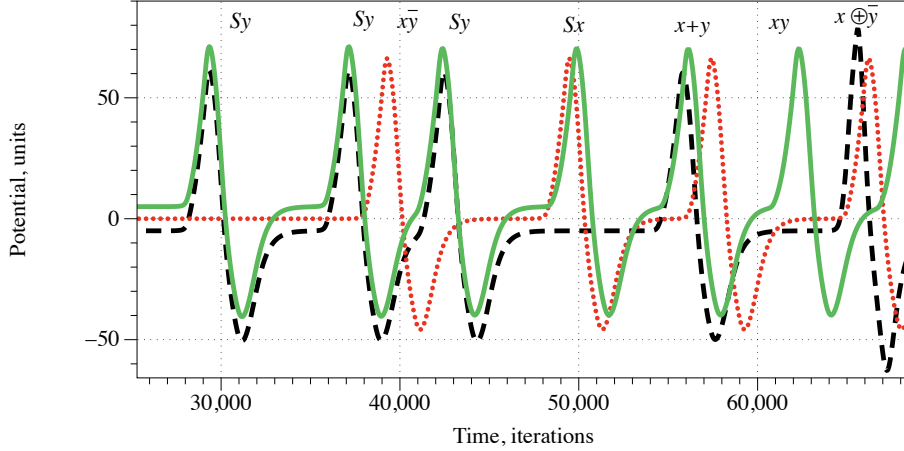


Figure 7: Fragment of electrical potential record on electrode 7 in response to inputs (01), black dashed line, (10), red dotted line, (11), solid green line, entered as impulses via electrodes $E_x = 5$ and $E_y = 15$. See locations of electrodes in Fig. 2d. To make the individual plots visible in places of exact overlapping, we added potential -5 to recording in response to input (01) and potential 5 to recording in response to input (11).

network, where they continue ‘circling’ indefinitely. A set of regular oscillations of activity becomes evidence after a number of iterations (Fig. 3d). The coverage of the network by excitation wave-fronts reduced with increase of c_2 from 0.095 to 0.096 (Fig. 6ab) and becomes localised when c_2 reaches 0.097 (Figs. 6c and 3b). Thus we used networks with $c_2 = 0.095$ or 0.096 for implementation of Boolean functions.

3.2. Distribution of Boolean gates

Input Boolean values are encoded as follows. We earmark two sites of the network as dedicated inputs, x and y , and represent logical TRUE, or ‘1’, as an excitation, or an impulse injected in the network via electrodes. If $x = 1$ then the site corresponding to x is excited, if $x = 0$ the site is not excited.

We here assume that each spike represents logical TRUE and that spikes occurring within less than $2 \cdot 10^2$ iterations happen simultaneously. By selecting specific intervals of recordings we can realise several gates in a single site of recording. In this particular case we assumed that spikes are separated if their occurrences lie more than 10^3 iterations apart. An example is shown in Fig. 7.

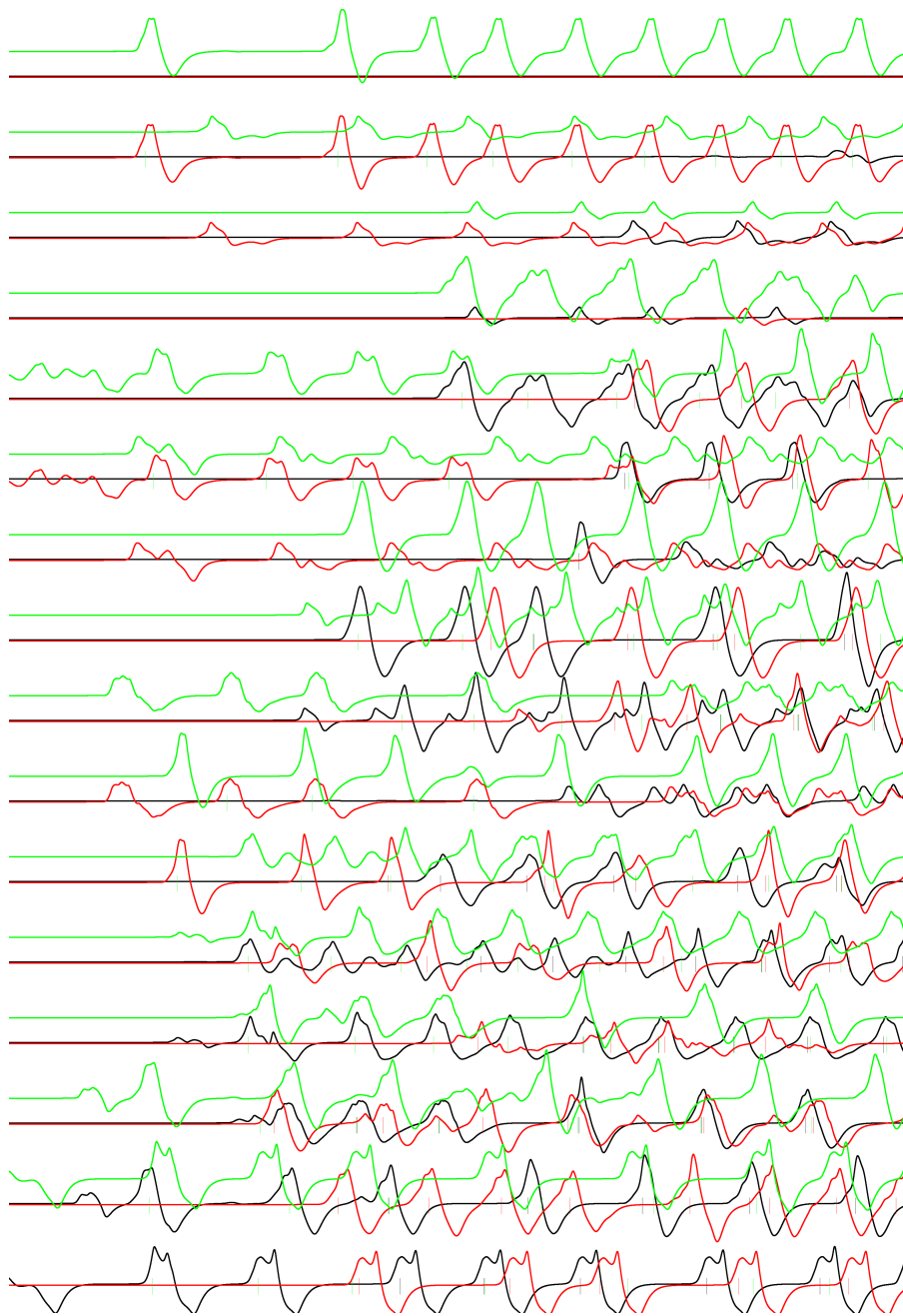


Figure 8: Recording of electrical potential from all electrodes in responses to inputs in response to inputs (01), black line, (10), red line, (11), green line, injected as spikes via electrodes $E_x = 5$ and $E_y = 15$.

| (a) $E_x = 3, E_y = 13, c_2 = 0.095$ | | | | | | | | (b) $E_x = 7, E_y = 14, c_2 = 0.095$ | | | | | | | | | |
|--------------------------------------|---------|------|--------------|------|------------|------------|------|--------------------------------------|-------|---------|------|--------------|------|------------|------------|------|-------|
| E | $x + y$ | Sy | $x \oplus y$ | Sx | $\bar{x}y$ | $x\bar{y}$ | xy | Total | E | $x + y$ | Sy | $x \oplus y$ | Sx | $\bar{x}y$ | $x\bar{y}$ | xy | Total |
| 0 | 0 | 0 | 0 | 0 | 0 | 0 | 0 | 0 | 0 | 0 | 0 | 0 | 0 | 0 | 0 | 0 | 0 |
| 1 | 0 | 0 | 0 | 2 | 0 | 0 | 0 | 2 | 1 | 0 | 0 | 5 | 0 | 0 | 0 | 0 | 5 |
| 2 | 0 | 0 | 0 | 0 | 0 | 0 | 0 | 0 | 2 | 0 | 0 | 0 | 0 | 0 | 0 | 0 | 0 |
| 3 | 0 | 0 | 0 | 0 | 0 | 0 | 0 | 0 | 3 | 0 | 0 | 0 | 0 | 0 | 0 | 0 | 0 |
| 4 | 1 | 0 | 0 | 7 | 1 | 0 | 0 | 9 | 4 | 0 | 0 | 6 | 1 | 0 | 0 | 7 | 7 |
| 5 | 0 | 0 | 0 | 2 | 2 | 0 | 0 | 4 | 5 | 0 | 0 | 6 | 0 | 0 | 0 | 6 | 6 |
| 6 | 0 | 0 | 0 | 2 | 0 | 0 | 0 | 2 | 6 | 0 | 0 | 2 | 0 | 0 | 0 | 2 | 2 |
| 7 | 1 | 0 | 0 | 8 | 2 | 0 | 0 | 11 | 7 | 1 | 0 | 4 | 2 | 0 | 0 | 7 | 7 |
| 8 | 1 | 0 | 0 | 6 | 1 | 0 | 0 | 8 | 8 | 0 | 0 | 7 | 0 | 0 | 0 | 7 | 7 |
| 9 | 0 | 0 | 0 | 0 | 1 | 0 | 0 | 1 | 9 | 0 | 0 | 0 | 0 | 0 | 0 | 0 | 0 |
| 10 | 0 | 1 | 1 | 2 | 0 | 1 | 2 | 7 | 10 | 1 | 0 | 1 | 5 | 0 | 0 | 7 | 7 |
| 11 | 0 | 0 | 0 | 4 | 2 | 0 | 0 | 6 | 11 | 1 | 0 | 0 | 4 | 3 | 0 | 8 | 8 |
| 12 | 0 | 0 | 0 | 3 | 2 | 0 | 0 | 5 | 12 | 2 | 0 | 0 | 3 | 0 | 0 | 5 | 5 |
| 13 | 1 | 5 | 0 | 0 | 0 | 1 | 0 | 7 | 13 | 1 | 5 | 0 | 1 | 0 | 2 | 0 | 9 |
| 14 | 2 | 5 | 0 | 1 | 0 | 1 | 0 | 9 | 14 | 0 | 4 | 0 | 2 | 1 | 2 | 1 | 10 |
| 15 | 0 | 1 | 0 | 5 | 2 | 0 | 0 | 8 | 15 | 0 | 0 | 0 | 8 | 2 | 0 | 0 | 10 |
| Total | 6 | 12 | 1 | 42 | 13 | 3 | 2 | 79 | Total | 6 | 9 | 1 | 53 | 9 | 4 | 1 | 83 |

| (c) $E_x = 7, E_y = 14, c_2 = 0.094$ | | | | | | | | (d) $E_x = 5, E_y = 15, c_2 = 0.094$ | | | | | | | | | |
|--------------------------------------|---------|------|--------------|------|------------|------------|------|--------------------------------------|-------|---------|------|--------------|------|------------|------------|------|-------|
| E | $x + y$ | Sy | $x \oplus y$ | Sx | $\bar{x}y$ | $x\bar{y}$ | xy | Total | E | $x + y$ | Sy | $x \oplus y$ | Sx | $\bar{x}y$ | $x\bar{y}$ | xy | Total |
| 0 | 0 | 0 | 0 | 0 | 0 | 0 | 0 | 0 | 0 | 0 | 0 | 0 | 0 | 0 | 0 | 0 | 0 |
| 1 | 0 | 0 | 0 | 2 | 1 | 0 | 0 | 3 | 1 | 0 | 0 | 0 | 1 | 1 | 0 | 0 | 2 |
| 2 | 0 | 0 | 0 | 0 | 0 | 0 | 0 | 0 | 2 | 0 | 0 | 0 | 0 | 0 | 0 | 0 | 0 |
| 3 | 0 | 0 | 0 | 0 | 0 | 0 | 0 | 0 | 3 | 0 | 0 | 0 | 0 | 0 | 0 | 0 | 0 |
| 4 | 0 | 0 | 0 | 1 | 3 | 0 | 0 | 4 | 4 | 0 | 1 | 0 | 0 | 2 | 1 | 1 | 5 |
| 5 | 0 | 0 | 0 | 1 | 1 | 0 | 0 | 2 | 5 | 0 | 0 | 0 | 0 | 1 | 0 | 0 | 1 |
| 6 | 0 | 0 | 0 | 1 | 1 | 0 | 0 | 2 | 6 | 0 | 0 | 0 | 0 | 1 | 0 | 0 | 1 |
| 7 | 0 | 0 | 0 | 0 | 2 | 0 | 0 | 2 | 7 | 1 | 2 | 0 | 0 | 0 | 4 | 0 | 7 |
| 8 | 0 | 0 | 0 | 3 | 4 | 0 | 0 | 7 | 8 | 0 | 1 | 0 | 1 | 2 | 1 | 0 | 5 |
| 9 | 0 | 0 | 0 | 0 | 1 | 2 | 0 | 3 | 9 | 0 | 0 | 0 | 1 | 2 | 0 | 0 | 3 |
| 10 | 0 | 0 | 0 | 1 | 1 | 0 | 0 | 2 | 10 | 0 | 0 | 0 | 2 | 0 | 0 | 1 | 3 |
| 11 | 0 | 0 | 0 | 0 | 6 | 0 | 0 | 6 | 11 | 1 | 5 | 0 | 0 | 1 | 1 | 1 | 9 |
| 12 | 1 | 0 | 1 | 2 | 3 | 1 | 0 | 8 | 12 | 0 | 6 | 0 | 0 | 1 | 2 | 0 | 9 |
| 13 | 0 | 2 | 0 | 2 | 0 | 1 | 0 | 5 | 13 | 2 | 0 | 2 | 1 | 1 | 1 | 1 | 8 |
| 14 | 1 | 3 | 0 | 0 | 3 | 0 | 2 | 9 | 14 | 0 | 1 | 0 | 1 | 0 | 5 | 0 | 7 |
| 15 | 0 | 2 | 0 | 0 | 0 | 1 | 0 | 3 | 15 | 0 | 0 | 0 | 0 | 0 | 1 | 0 | 1 |
| Total | 2 | 7 | 1 | 13 | 26 | 5 | 2 | 56 | Total | 4 | 16 | 2 | 7 | 12 | 16 | 4 | 61 |

| (e) $E_x = 5, E_y = 15, c_2 = 0.095$ | | | | | | | | (f) $E_x = 5, E_y = 15, c_2 = 0.096$ | | | | | | | | | |
|--------------------------------------|---------|------|--------------|------|------------|------------|------|--------------------------------------|-------|---------|------|--------------|------|------------|------------|------|-------|
| E | $x + y$ | Sy | $x \oplus y$ | Sx | $\bar{x}y$ | $x\bar{y}$ | xy | Total | E | $x + y$ | Sy | $x \oplus y$ | Sx | $\bar{x}y$ | $x\bar{y}$ | xy | Total |
| 0 | 0 | 0 | 0 | 0 | 0 | 0 | 0 | 0 | 0 | 0 | 0 | 0 | 0 | 0 | 0 | 0 | 0 |
| 1 | 0 | 0 | 0 | 8 | 0 | 0 | 0 | 8 | 1 | 0 | 0 | 0 | 2 | 1 | 0 | 0 | 3 |
| 2 | 0 | 0 | 0 | 0 | 0 | 0 | 0 | 0 | 2 | 0 | 0 | 0 | 0 | 0 | 0 | 0 | 0 |
| 3 | 0 | 0 | 0 | 0 | 0 | 0 | 0 | 0 | 3 | 0 | 0 | 0 | 0 | 0 | 0 | 0 | 0 |
| 4 | 1 | 4 | 0 | 0 | 0 | 2 | 0 | 7 | 4 | 1 | 3 | 0 | 0 | 0 | 1 | 0 | 5 |
| 5 | 3 | 0 | 0 | 4 | 0 | 0 | 0 | 7 | 5 | 0 | 0 | 0 | 4 | 2 | 0 | 0 | 6 |
| 6 | 0 | 0 | 0 | 0 | 1 | 0 | 0 | 1 | 6 | 0 | 0 | 0 | 2 | 1 | 0 | 0 | 3 |
| 7 | 1 | 3 | 1 | 1 | 0 | 1 | 1 | 8 | 7 | 1 | 4 | 0 | 1 | 0 | 1 | 0 | 7 |
| 8 | 0 | 5 | 0 | 1 | 0 | 2 | 0 | 8 | 8 | 1 | 5 | 0 | 0 | 0 | 1 | 0 | 7 |
| 9 | 0 | 0 | 0 | 3 | 0 | 0 | 0 | 3 | 9 | 0 | 0 | 0 | 7 | 0 | 0 | 0 | 7 |
| 10 | 1 | 0 | 2 | 4 | 2 | 0 | 2 | 11 | 10 | 0 | 1 | 0 | 5 | 1 | 1 | 0 | 8 |
| 11 | 2 | 4 | 0 | 2 | 2 | 0 | 1 | 11 | 11 | 2 | 3 | 0 | 1 | 1 | 1 | 1 | 9 |
| 12 | 1 | 7 | 0 | 0 | 0 | 3 | 0 | 11 | 12 | 0 | 4 | 0 | 0 | 0 | 0 | 0 | 4 |
| 13 | 3 | 1 | 0 | 2 | 0 | 1 | 0 | 7 | 13 | 0 | 2 | 0 | 2 | 0 | 2 | 0 | 6 |
| 14 | 1 | 5 | 0 | 0 | 0 | 6 | 0 | 12 | 14 | 1 | 3 | 0 | 2 | 0 | 3 | 0 | 9 |
| 15 | 1 | 3 | 1 | 2 | 2 | 1 | 1 | 11 | 15 | 0 | 3 | 0 | 2 | 0 | 2 | 0 | 7 |
| Total | 14 | 32 | 4 | 27 | 7 | 16 | 5 | 105 | Total | 6 | 28 | 0 | 28 | 6 | 12 | 1 | 81 |

Table 1: Numbers of Boolean gates detected for selected pairs of input electrodes E_x and E_y .

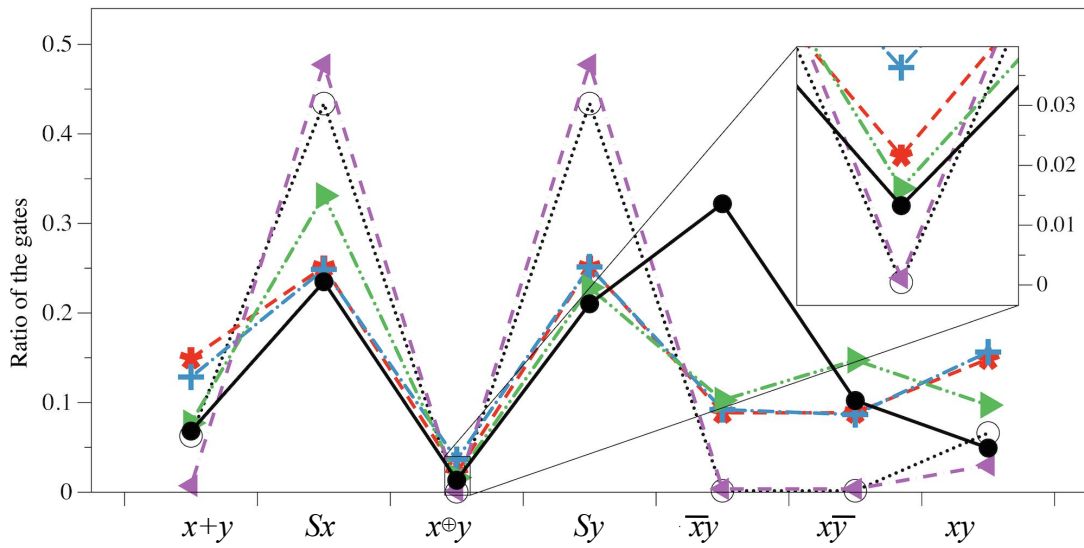


Figure 9: Comparative ratios of Boolean gates discovered in mycelium network in present analysed in present paper, black disc and solid line; slime mould *Physarum polycephalum* [34], black circle and dotted line; succulent plant [11], red snowflake and dashed line; single molecule of protein verotoxin [2], light blue '+' and dash-dot line; actin bundles network [12], green triangle pointing right and dash-dot-dot line; actin monomer [3], magenta triangle pointing left and dashed line. Area of XOR gate is magnified in the insert. Lines are to guide eye only.

Numbers of Boolean gates detected on the electrodes for selected pairs of input electrodes are shown in Tab. 1. We see that select x and select y gates, Sx and Sy are most frequent. They usually are detected with the same frequency (Tab. 1d–f), however there are examples of input electrode pairs, where one of the select gates is found much more often than another. This is most visible for the pair $(E_x, E_y) = (3, 13)$ where Sx dominates (Tab. 1a), and the pair (7,14) and (Tab. 1bc) where Sy dominates. Next common gates in the hierarchy are $\bar{x}y$ and $x\bar{y}$. The gates xy and $x + y$ are detected with nearly the same frequency with gate $x + y$ being slightly more common. The $x \oplus y$ is the most rare gate.

The sub-tables Tab. 1d, Tab. 1e and Tab. 1f show how excitability of the network affects numbers of gates detected. The networks with high excitability, $c_2 = 0.094$, and low excitability, $c_2 = 0.0096$ realise smaller number of gates than that realised by sub-excitable network, $c_2 = 0.095$.

Overall distribution (average of outputs of input electrode pairs (3,13), (5,15), (7,14), (4,13), (13,7)) of a ratio of gates discovered is shown in Fig. 9. This is accompanied by distributions of gates discovered in experimental laboratory reservoir computing with slime mould *Physarum polycephalum* [34], succulent plant [11] and numerical modelling experiments on computing with protein verotoxin [2], actin bundles network [12], and actin monomer [3]. All the listed distributions have very similar structure with gates selecting one of the inputs in majority, followed by OR gate, NOT-AND and AND-NOT gates. The gate AND is usually underrepresented in experimental and modelling experiments. The gate XOR is a rare find.

4. Discussion

We have demonstrated how sets of logical gates can be implemented in single colony mycelium networks via initiation of electrical impulses. The impulses travel in the network, interact with each other (annihilate, reflect, change their phase). Thus for different combinations of input impulses and record different combinations of output impulses, which in some cases can be interpreted as representing two-inputs-one-output functions.

To estimate a speed of computation we refer to Olsson and Hansson’s [54] original study, in which they proposed that electrical activity in fungi could be used for communication with message propagation speed 0.5 mm/sec. Diameter of the colony (Fig. 2a), which experimental laboratory images has been used to run FHN model, is c. 1.7 mm. Thus, it takes the excitation

waves initiated at a boundary of the colony up to 3-4 sec to span the whole mycelium network (this time is equivalent to c. 70K iterations of the numerical integration model). In 3-4 sec the mycelium network can compute up to a hundred logical gates. This gives us the rate of a gate per 0.03 sec, or, in terms of frequency this will be c. 30 Hz. The mycelium network computing can not compete with existing silicon architecture however its application domain can be a unique of living biosensors (a distribution of gates realised might be affected by environmental conditions) [44] and computation embedded into structural elements where fungal materials are used [61, 35, 17].

5. Acknowledgement

This project has received funding from the European Union’s Horizon 2020 research and innovation programme FET OPEN “Challenging current thinking” under grant agreement No 858132.

References

References

- [1] Andrew Adamatzky. Collision-based computing in Belousov–Zhabotinsky medium. *Chaos, Solitons & Fractals*, 21(5):1259–1264, 2004.
- [2] Andrew Adamatzky. Computing in verotoxin. *ChemPhysChem*, 18(13):1822–1830, 2017.
- [3] Andrew Adamatzky. Logical gates in actin monomer. *Scientific reports*, 7(1):1–14, 2017.
- [4] Andrew Adamatzky. On spiking behaviour of oyster fungi pleurotus djamor. *Scientific reports*, 8(1):1–7, 2018.
- [5] Andrew Adamatzky. On interplay between excitability and geometry. *arXiv preprint arXiv:1904.06526*, 2019.
- [6] Andrew Adamatzky. Plant leaf computing. *Biosystems*, 2019.
- [7] Andrew Adamatzky, Ben de Lacy Costello, and Larry Bull. On polymorphic logical gates in subexcitable chemical medium. *International Journal of Bifurcation and Chaos*, 21(07):1977–1986, 2011.

- [8] Andrew Adamatzky, Ben De Lacy Costello, Larry Bull, and Julian Holley. Towards arithmetic circuits in sub-excitable chemical media. *Israel Journal of Chemistry*, 51(1):56–66, 2011.
- [9] Andrew Adamatzky and Benjamin de Lacy Costello. Binary collisions between wave-fragments in a sub-excitable Belousov–Zhabotinsky medium. *Chaos, Solitons & Fractals*, 34(2):307–315, 2007.
- [10] Andrew Adamatzky, Benjamin de Lacy Costello, Chris Melhuish, and Norman Ratcliffe. Experimental implementation of mobile robot taxis with onboard Belousov–Zhabotinsky chemical medium. *Materials Science and Engineering: C*, 24(4):541–548, 2004.
- [11] Andrew Adamatzky, Simon Harding, Victor Erokhin, Richard Mayne, Nina Gizzie, Frantisek Baluška, Stefano Mancuso, and Georgios Ch Sirakoulis. Computers from plants we never made: Speculations. In *Inspired by nature*, pages 357–387. Springer, 2018.
- [12] Andrew Adamatzky, Florian Huber, and Jörg Schnauß. Computing on actin bundles network. *Scientific reports*, 9(1):1–10, 2019.
- [13] Andrew Adamatzky, Martin Tegelaar, Han Wosten, Anna Powell, and Alexander Beasley. Supplementary materials. on boolean gates in fungal colony.
- [14] Go W Beeler and H Reuter. Reconstruction of the action potential of ventricular myocardial fibres. *The Journal of physiology*, 268(1):177–210, 1977.
- [15] Lynne Boddy, John M Wells, Claire Culshaw, and Damian P Donnelly. Fractal analysis in studies of mycelium in soil. *Geoderma*, 88(3):301–328, 1999.
- [16] Rory G Bolton and Lynne Boddy. Characterization of the spatial aspects of foraging mycelial cord systems using fractal geometry. *Mycological research*, 97(6):762–768, 1993.
- [17] Joseph Dahmen. Soft matter: Responsive architectural operations. *Technoetic Arts*, 14(1-2):113–125, 2016.

- [18] Matthew Dale, Julian F Miller, and Susan Stepney. Reservoir computing as a model for in-materio computing. In *Advances in Unconventional Computing*, pages 533–571. Springer, 2017.
- [19] Matthew Dale, Julian F Miller, Susan Stepney, and Martin A Trefzer. A substrate-independent framework to characterize reservoir computers. *Proceedings of the Royal Society A*, 475(2226):20180723, 2019.
- [20] Ben de Lacy Costello, Rita Toth, Christopher Stone, Andrew Adamatzky, and Larry Bull. Implementation of glider guns in the light-sensitive Belousov-Zhabotinsky medium. *Physical Review E*, 79(2):026114, 2009.
- [21] Ronald P De Vries, Kim Burgers, Peter JI van de Vondervoort, Jens C Frisvad, Robert A Samson, and Jaap Visser. A new black aspergillus species, *a. vadensis*, is a promising host for homologous and heterologous protein production. *Appl. Environ. Microbiol.*, 70(7):3954–3959, 2004.
- [22] Richard FitzHugh. Impulses and physiological states in theoretical models of nerve membrane. *Biophysical journal*, 1(6):445–466, 1961.
- [23] M Fricker, L Boddy, and D Bebbber. Network organisation of mycelial fungi. In *Biology of the fungal cell*, pages 309–330. Springer, 2007.
- [24] Mark D Fricker, Luke LM Heaton, Nick S Jones, and Lynne Boddy. The mycelium as a network. *The Fungal Kingdom*, pages 335–367, 2017.
- [25] Jörg Fromm. Control of phloem unloading by action potentials in *mimosa*. *Physiologia Plantarum*, 83(3):529–533, 1991.
- [26] Jörg Fromm and Silke Lautner. Electrical signals and their physiological significance in plants. *Plant, cell & environment*, 30(3):249–257, 2007.
- [27] Pier Luigi Gentili, Viktor Horvath, Vladimir K Vanag, and Irving R Epstein. Belousov-Zhabotinsky “chemical neuron” as a binary and fuzzy logic processor. *IJUC*, 8(2):177–192, 2012.
- [28] Manuela Giovannetti, Cristiana Sbrana, Luciano Avio, and Patrizia Strani. Patterns of below-ground plant interconnections established by means of arbuscular mycorrhizal networks. *New Phytologist*, 164(1):175–181, 2004.

- [29] Jerzy Gorecki and Joanna Natalia Gorecka. Information processing with chemical excitations—from instant machines to an artificial chemical brain. *International Journal of Unconventional Computing*, 2(4), 2006.
- [30] Jerzy Gorecki, Joanna Natalia Gorecka, and Yasuhiro Igarashi. Information processing with structured excitable medium. *Natural Computing*, 8(3):473–492, 2009.
- [31] Gerd Gruenert, Konrad Gizynski, Gabi Escuela, Bashar Ibrahim, Jerzy Gorecki, and Peter Dittrich. Understanding networks of computing chemical droplet neurons based on information flow. *International journal of neural systems*, 25(07):1450032, 2015.
- [32] Shan Guo, Ming-Zhu Sun, and Xin Han. Digital comparator in excitable chemical media. *International Journal Unconventional Computing*, 2015.
- [33] Peter Hammer. Spiral waves in monodomain reaction-diffusion model, 2009.
- [34] Simon Harding, Jan Koutník, Jürgen Schmidhuber, and Andrew Adamatzky. Discovering boolean gates in slime mould. In *Inspired by Nature*, pages 323–337. Springer, 2018.
- [35] Felix Heisel, Juney Lee, Karsten Schlesier, Matthias Rippmann, Nazanin Saeidi, Alireza Javadian, Adi Reza Nugroho, Tom Van Mele, Philippe Block, and Dirk E Hebel. Design, cultivation and application of load-bearing mycelium components. *International Journal of Sustainable Energy Development*, 6(2), 2018.
- [36] D Hitchcock, CA Glasbey, and K Ritz. Image analysis of space-filling by networks: Application to a fungal mycelium. *Biotechnology Techniques*, 10(3):205–210, 1996.
- [37] Yasuhiro Igarashi and Jerzy Gorecki. Chemical diodes built with controlled excitable media. *IJUC*, 7(3):141–158, 2011.
- [38] MR Islam, G Tudryn, R Bucinell, L Schadler, and RC Picu. Morphology and mechanics of fungal mycelium. *Scientific reports*, 7(1):1–12, 2017.

- [39] Tatsuichi Iwamura. Correlations between protoplasmic streaming and bioelectric potential of a slime mold, *Physarum polycephalum*. *Shokubutsugaku Zasshi*, 62(735-736):126–131, 1949.
- [40] Noburo Kamiya and Shigemi Abe. Bioelectric phenomena in the myxomycete plasmodium and their relation to protoplasmic flow. *Journal of Colloid Science*, 5(2):149–163, 1950.
- [41] U Kishimoto. Rhythmicity in the protoplasmic streaming of a slime mold, *Physarum polycephalum*. I. a statistical analysis of the electric potential rhythm. *The Journal of general physiology*, 41(6):1205–1222, 1958.
- [42] Zoran Konkoli, Stefano Nichele, Matthew Dale, and Susan Stepney. Reservoir computing with computational matter. In *Computational Matter*, pages 269–293. Springer, 2018.
- [43] Mantas Lukoševičius and Herbert Jaeger. Reservoir computing approaches to recurrent neural network training. *Computer Science Review*, 3(3):127–149, 2009.
- [44] Veronica Manzella, Claudio Gaz, Andrea Vitaletti, Elisa Masi, Luisa Santopolo, Stefano Mancuso, D Salazar, and JJ De Las Heras. Plants as sensing devices: the PLEASED experience. In *Proceedings of the 11th ACM conference on embedded networked sensor systems*, pages 1–2, 2013.
- [45] R Meyer and W Stockem. Studies on microplasmodia of *Physarum polycephalum* V: electrical activity of different types of microplasmodia and macroplasmodia. *Cell biology international reports*, 3(4):321–330, 1979.
- [46] JD Mihail, M Obert, JN Bruhn, and SJ Taylor. Fractal geometry of diffuse mycelia and rhizomorphs of armillaria species. *Mycological Research*, 99(1):81–88, 1995.
- [47] Julian F Miller and Keith Downing. Evolution in materio: Looking beyond the silicon box. In *Proceedings 2002 NASA/DoD Conference on Evolvable Hardware*, pages 167–176. IEEE, 2002.

- [48] Julian F Miller, Simon L Harding, and Gunnar Tuftte. Evolution-in-materio: evolving computation in materials. *Evolutionary Intelligence*, 7(1):49–67, 2014.
- [49] Julian F Miller, Simon J Hickinbotham, and Martyn Amos. In materio computation using carbon nanotubes. In *Computational Matter*, pages 33–43. Springer, 2018.
- [50] Julian Francis Miller. The alchemy of computation: designing with the unknown. *Natural Computing*, 18(3):515–526, 2019.
- [51] PV Minorsky. Temperature sensing by plants: a review and hypothesis. *Plant, Cell & Environment*, 12(2):119–135, 1989.
- [52] Jinichi Nagumo, Suguru Arimoto, and Shuji Yoshizawa. An active pulse transmission line simulating nerve axon. *Proceedings of the IRE*, 50(10):2061–2070, 1962.
- [53] M Obert, P Pfeifer, and M Sernetz. Microbial growth patterns described by fractal geometry. *Journal of Bacteriology*, 172(3):1180–1185, 1990.
- [54] S Olsson and BS Hansson. Action potential-like activity found in fungal mycelia is sensitive to stimulation. *Naturwissenschaften*, 82(1):30–31, 1995.
- [55] Maria Papagianni. Quantification of the fractal nature of mycelial aggregation in aspergillus niger submerged cultures. *Microbial Cell Factories*, 5(1):5, 2006.
- [56] Dhananjay B Patankar, Tuan-Chi Liu, and Timothy Oolman. A fractal model for the characterization of mycelial morphology. *Biotechnology and bioengineering*, 42(5):571–578, 1993.
- [57] Arkady M Pertsov, Jorge M Davidenko, Remy Salomonsz, William T Baxter, and Jose Jalife. Spiral waves of excitation underlie reentrant activity in isolated cardiac muscle. *Circulation research*, 72(3):631–650, 1993.
- [58] Barbara G Pickard. Action potentials in higher plants. *The Botanical Review*, 39(2):172–201, 1973.

- [59] G Roblin. Analysis of the variation potential induced by wounding in plants. *Plant and cell physiology*, 26(3):455–461, 1985.
- [60] Jack M Rogers and Andrew D McCulloch. A collocation-Galerkin finite element model of cardiac action potential propagation. *IEEE Transactions on Biomedical Engineering*, 41(8):743–757, 1994.
- [61] Philip Ross. Your rotten future will be great. *The Routledge Companion to Biology in Art and Architecture*, page 252, 2016.
- [62] Johannes Schindelin, Ignacio Arganda-Carreras, Erwin Frise, Verena Kaynig, Mark Longair, Tobias Pietzsch, Stephan Preibisch, Curtis Rueden, Stephan Saalfeld, Benjamin Schmid, et al. Fiji: an open-source platform for biological-image analysis. *Nature methods*, 9(7):676–682, 2012.
- [63] Takao Sibaoka. Rapid plant movements triggered by action potentials. *The botanical magazine= Shokubutsu-gaku-zasshi*, 104(1):73–95, 1991.
- [64] Jakub Siewewiesiuk and Jerzy Górecki. Logical functions of a cross junction of excitable chemical media. *The Journal of Physical Chemistry A*, 105(35):8189–8195, 2001.
- [65] PJ Simons. The role of electricity in plant movements. *New Phytologist*, 87(1):11–37, 1981.
- [66] Clifford L Slayman, W Scott Long, and Dietrich Gradmann. “Action potentials” in *Neurospora crassa*, a mycelial fungus. *Biochimica et Biophysica Acta (BBA) — Biomembranes*, 426(4):732–744, 1976.
- [67] Oliver Steinbock, Petteri Kettunen, and Kenneth Showalter. Chemical wave logic gates. *The Journal of Physical Chemistry*, 100(49):18970–18975, 1996.
- [68] Susan Stepney. Co-designing the computational model and the computing substrate. In *International Conference on Unconventional Computation and Natural Computation*, pages 5–14. Springer, 2019.
- [69] William M Stevens, Andrew Adamatzky, Ishrat Jahan, and Ben de Lacy Costello. Time-dependent wave selection for information processing in excitable media. *Physical Review E*, 85(6):066129, 2012.

- [70] James Stovold and Simon O’Keefe. Simulating neurons in reaction-diffusion chemistry. In *International Conference on Information Processing in Cells and Tissues*, pages 143–149. Springer, 2012.
- [71] Ming-Zhu Sun and Xin Zhao. Multi-bit binary decoder based on Belousov-Zhabotinsky reaction. *The Journal of chemical physics*, 138(11):114106, 2013.
- [72] Ming-Zhu Sun and Xin Zhao. Crossover structures for logical computations in excitable chemical medium. *International Journal Unconventional Computing*, 2015.
- [73] Hisako Takigawa-Imamura and Ikuko N Motoike. Dendritic gates for signal integration with excitability-dependent responsiveness. *Neural Networks*, 24(10):1143–1152, 2011.
- [74] Rita Toth, Christopher Stone, Ben de Lacy Costello, Andrew Adamatzky, and Larry Bull. Simple collision-based chemical logic gates with adaptive computing. *Theoretical and Technological Advancements in Nanotechnology and Molecular Computation: Interdisciplinary Gains: Interdisciplinary Gains*, page 162, 2010.
- [75] Kazimierz Trebacz, Halina Dziubinska, and Elzbieta Krol. Electrical signals in long-distance communication in plants. In *Communication in plants*, pages 277–290. Springer, 2006.
- [76] Alejandro Vazquez-Otero, Jan Faigl, Natividad Duro, and Raquel Dormido. Reaction-diffusion based computational model for autonomous mobile robot exploration of unknown environments. *IJUC*, 10(4):295–316, 2014.
- [77] David Verstraeten, Benjamin Schrauwen, Michiel d’Haene, and Dirk Stroobandt. An experimental unification of reservoir computing methods. *Neural networks*, 20(3):391–403, 2007.
- [78] Arman Vinck, Charissa de Bekker, Adam Ossin, Robin A Ohm, Ronald P de Vries, and Han AB Wösten. Heterogenic expression of genes encoding secreted proteins at the periphery of *Aspergillus niger* colonies. *Environmental microbiology*, 13(1):216–225, 2011.

- [79] Alexander G Volkov. Green plants: electrochemical interfaces. *Journal of Electroanalytical Chemistry*, 483(1-2):150–156, 2000.
- [80] Alexander G Volkov, Justin C Foster, Talitha A Ashby, Ronald K Walker, Jon A Johnson, and Vladislav S Markin. Mimosa pudica: electrical and mechanical stimulation of plant movements. *Plant, cell & environment*, 33(2):163–173, 2010.
- [81] Hiroshi Yokoi, Andy Adamatzky, Ben de Lacy Costello, and Chris Melhuish. Excitable chemical medium controller for a robotic hand: Closed-loop experiments. *International Journal of Bifurcation and Chaos*, 14(09):3347–3354, 2004.
- [82] Guo-Mao Zhang, Jeong Wong, Meng-Ta Chou, and Xin Zhao. Towards constructing multi-bit binary adder based on Belousov-Zhabotinsky reaction. *The Journal of chemical physics*, 136(16):164108, 2012.
- [83] Matthias R Zimmermann and Axel Mithöfer. Electrical long-distance signaling in plants. In *Long-Distance Systemic Signaling and Communication in Plants*, pages 291–308. Springer, 2013.